

Electric field gradient effects in Raman spectroscopy

E. J. Ayars, H. D. Hallen

Physics Department, North Carolina State University, Raleigh, NC 27695-8202

C. L. Jahncke

Physics Department, St. Lawrence University, Canton, NY 13617

Abstract

Raman spectra of materials subject to strong electric field gradients, such as those present near a metal surface, can show significantly altered selection rules. We describe a new mechanism by which the field gradients can produce Raman-like lines. We develop a theoretical model for this “Gradient-Field Raman” effect, discuss selection rules, and compare to other mechanisms that produce Raman-like lines in the presence of strong field gradients. The mechanism can explain the origin and intensity of some Raman modes observed in SERS and through a Near-Field Optical Microscope (NSOM-Raman).

PACS Numbers: 33.20.Fb, 78.30.-j, 78.66.Vs, 82.80.Ch

The proximity of metallic structures to a sample has profound effects on the Raman spectra of that sample. It leads to surface enhanced Raman spectroscopy (SERS), for example see [1, 2] and references within, and also to differences between far-field and near-field Raman spectroscopy measured with a near-field optical microscope (NSOM). [3-5] Two aspects of the spectra, the selection rules and the mode intensities, are altered by the presence of the metal. We concentrate in this paper on selection rule changes. The selection rules can be altered by the change of symmetry due to the image charge in the metal, [6] a change in site symmetry with surface bonding, [7-9] or due to the nature of the electric field. An internal electric field has been shown to change Raman selection rules in semiconductors that lack a center of symmetry. [10-12] When the gradient of the electric field is large, such as at a metallic surface, selection rules can be modified. [13-15]

We describe an alternative method through which a strong gradient of the electric field can alter the Raman spectra, and investigate its implications on selection rules. When an electric field varies over the length of a bond, a Raman signal can be generated that depends upon the polarizability times the field gradient rather than the field times the polarizability gradient. The field gradient shifts the potential energy of the induced dipole in an asymmetric manner, leading to a coupling with the applied field and hence emission or absorption of phonons. The selection rules for this process, which we term gradient-field Raman (GFR), depend upon the bond orientation, with relative intensities resembling those of infrared spectroscopy. They differ markedly from the usual Raman selection rules.

Transitions in vibration levels due to coupling with a radiation field are described by the perturbation Hamiltonian $H = -\boldsymbol{\mu} \cdot \mathbf{E}$, where $\boldsymbol{\mu}$ is the dipole moment and \mathbf{E} is the electric field. [16] The dipole moment can be written as

$$\mu_a = \mu_a^p + \alpha_{ab} E_b + \frac{1}{3} A_{abc} \frac{\partial E_b}{\partial c} + G_{ab} B_b + \dots, \quad (1)$$

where the $\{a,b,c\}$ are a permutation of the coordinates $\{x,y,z\}$ (summing over repeated indices is implied), μ^p is the permanent dipole moment, B is the magnetic field, and α is the polarizability

tensor. The α , A, and G are given in Ref. [13]. The derivation of the spectroscopic signals proceeds with a first order expansion of μ in the coordinate of vibration Q:

$$\begin{aligned} \mu_a = & (\mu_a^p)_0 + \left(\frac{d\mu_a^p}{dQ}\right)_0 Q + (\alpha_{ab}E_b)_0 + \left(\frac{d\alpha_{ab}E_b}{dQ}\right)_0 Q + \frac{1}{3} \frac{\partial E_b}{\partial c} \left\{ (A_{abc})_0 + \left(\frac{dA_{abc}}{dQ}\right)_0 Q \right\} \\ & + (G_{ab}B_b)_0 + \left(\frac{dG_{ab}B_b}{dQ}\right)_0 Q + \dots \end{aligned} \quad (2)$$

The terms without Q dependence (1st, 3rd, etc.) are discarded since they will not couple adjacent vibration states. The second term yields the direct photon absorption (infrared spectroscopy). Raman spectroscopy derives from the fourth term. Usually the electric field is assumed to be independent of Q and hence is removed from the derivative. Since the field can vary very rapidly near a metal surface, [17] we do not remove it from the derivative. The extra term that results is our ‘gradient field Raman’ term. The sixth term has been discussed before, and can also be important when the field varies rapidly, such as near a metal surface. [13-15] The remaining terms are small even in high field-gradient regions and can be neglected. The relevant dipole terms can thus be written as:

$$\mu_a = \left\{ \left(\frac{d\mu_a^p}{dQ}\right)_0 + \left(\frac{d\alpha_{ab}}{dQ}\right)_0 E_b + \alpha_{ab} \left(\frac{dE_b}{dQ}\right)_0 + \frac{1}{3} \frac{\partial E_b}{\partial c} \left(\frac{dA_{abc}}{dQ}\right)_0 \right\} Q. \quad (3)$$

The four terms result in IR absorption, Raman, GFR, and quadrupole-Raman. The ratio of the GFR term to the Raman term depends upon the field gradient and the polarizability gradient, which we approximate as α/a , where a is close to an atomic dimension. In vacuum, the field gradient yields terms of the order $i(2\pi/\lambda)E_b$. Near a metal surface, the jellium approximation of Feibelman [17] indicates that the electric field varies by nearly its full amplitude over a distance of 0.2 nm. The derivative is then approximately $E_b/0.2$ nm. The ratio of the GFR term/Raman term in vacuum is of order $2\pi a/\lambda$. For 500 nm light and $a = 0.2$ nm, this is $\sim 10^{-3}$, so that the GFR contribution is insignificant. The situation is different near a metal surface, where the ratio of the GFR term/Raman term is $a/0.2$ nm, or ~ 1 . We thus expect to find a measurable GFR signal near metal surfaces.

As in the usual Raman spectroscopy, the GFR effect is observed as a shift in the energy of photons. This can be seen by writing the polarization as a first order expansion of both the electric field and polarizability $P = \alpha E_b \cos\omega t$ in terms of $Q = Q_0 \cos\omega_v t$, as above.

$$\begin{aligned} P = \alpha E_b \cos\omega t & = \left(\alpha_0 + \left(\frac{d\alpha}{dQ}\right)_0 Q \right) \left(E_0 + \left(\frac{dE}{dQ}\right)_0 Q \right) \cos\omega t \\ & = \alpha_0 E_0 \cos\omega t + \frac{1}{2} Q_0 \left(\frac{d\alpha}{dQ}\right)_0 E_0 \{ \cos[(\omega - \omega_v)t] + \cos[(\omega + \omega_v)t] \} \\ & \quad + \frac{1}{2} Q_0 \left(\frac{dE}{dQ}\right)_0 \alpha_0 \{ \cos[(\omega - \omega_v)t] + \cos[(\omega + \omega_v)t] \}, \end{aligned} \quad (4)$$

The Raman and GFR terms show oscillations at the incident frequency plus or minus the vibration frequency, $\cos(\omega \pm \omega_v)t$. These correspond to the anti-Stokes and Stokes modes, respectively. The strong similarity in this derivation to that of Raman spectroscopy leads us to name the effect as a type of Raman (Gradient-Field Raman) spectroscopy.

The GFR differs appreciably from Raman spectroscopy in selection rules. Selection rules result from the requirement that $\langle \psi_f | \mu \cdot E | \psi_i \rangle$ be nonzero. The Q dependence of μ , Eqn. 3, means that this expectation will be nonzero if the ψ differ by one vibration quantum; also, the coefficient of Q in Eqn. 3 must also be nonzero. The Raman selection rules are determined by

the requirement that $d\alpha/dQ$ be nonzero at $Q = 0$. This is equivalent to the condition that α and the vibration belong to the same symmetry species. [18] Conversely, the GFR selection rules require that E belong to the same symmetry species as the vibration, or that dE/dQ be nonzero at $Q = 0$. This will be true if the vibration has a component normal to the surface, since that is the direction in which E varies rapidly. For a flat surface, the selection rules resemble 'surface selection rules,' [6] although surface roughness will allow other modes. The polarizability must also be nonzero: for example, if z is normal to the surface, then α_{az} and E_a must be nonzero for some a in $\{x, y, z\}$. This is the case for NSOM, which has most components of \mathbf{E} near the probe, [19] but can be limiting in far-field measurements. The polarizability influences the magnitude of the effect, since it multiplies the derivative. The GFR effect should be large when the polarizability is large, such as for ionic bonding. This is in contrast to Raman spectroscopy, which typically is stronger for covalent bonding. Infrared spectroscopy is strongest for ionic bonding, however, so (for infrared allowed lines) the GFR effects should be strongest for the vibration modes for which infrared absorption is strong (although GFR may also be strong for non-IR-allowed vibrations). This means that some GFR lines can complement the Raman spectra if a strong field gradient is applied along the vibrating bond.

Most of the Raman work (except NSOM) performed near metal surfaces has been concerned with SERS. We do not comment on SERS models here, but note which peaks not normally seen in Raman are expressed. In particular, when the strong new lines involve strong IR vibrations, it suggests that GFR is important. Surface effects, for the rough surfaces typically used for SERS, must also be included in the analysis of the selection rules. When the spectra is minimally impacted by the surface, indicated by Raman energies unperturbed from the bulk material, new active modes probably result from GFR or the quadrupole term rather than symmetry changes or bonding. The presence of GFR induced lines cannot be proved, since particular scenarios could cause these 'GFR preferred' lines to be strong even if another mechanism altered the selection rules. However, strong circumstantial evidence for GFR results from the presence of normally forbidden modes and their relative strength of compared to bulk IR strength, corrected for orientation with respect to the surface.

Benzene has been studied extensively with the SERS technique, on several roughened metal surfaces. [20-22] The general findings are that many normally Raman forbidden modes are observed. Whereas these could be understood from symmetry changes upon interacting with the surface, [20] the shifts of the Raman allowed modes from the bulk are small when bonded to silver, [20] and even smaller when bonded to sodium. [21, 22] It is therefore unlikely that the interaction with the substrate is sufficient to describe the appearance of the lines. Of the modes normally allowed in gas-phase IR, [22] the 692 cm^{-1} line, the most intense line of the IR spectrum, was also the most intense of these lines in the Raman spectrum. Of the modes usually not allowed in either Raman or gas-phase IR, [22] the 403 cm^{-1} e_{2u} mode was the strongest observed, although the e_{2g} mode at 976 cm^{-1} and the b_{2u} modes at 1313 cm^{-1} and 1148 cm^{-1} were also seen. These modes are all seen in liquid-phase IR spectroscopy, in which the 403 cm^{-1} mode is strong, and the latter three are weak. [23] These intensities all agree with what one would expect for a GFR-related effect. Further, of the five out-of-plane vibrations, three were observed to be selectively enhanced (the only selectively enhanced modes), and the other two are not IR active in the gas or the liquid phase. If the benzene lies flat on the surface, as has been suggested, [22] these would be the modes sensing the most electric field gradient in GFR.

Other molecules studied on metal surfaces include $\text{Ru}(\text{CN})_6^{4-}$ on Ag and Cu. [24] Both show significant contributions from the strong IR vibrations near 550 cm^{-1} and 2048 cm^{-1} . The 550 cm^{-1} mode involves the motion of several CN's to-and-from the surface, so the GFR model correctly anticipates its large intensity. The 365 cm^{-1} IR mode, on the other hand, is observed weakly in both the silver and the more strongly interacting Cu cases. The C_{60} molecule has been placed on Ag and Au surfaces with minimal surface interactions, as gauged by Raman line shifts. Nevertheless, modes normally only IR active are observed in the spectra. [25, 26] Finally, 2-

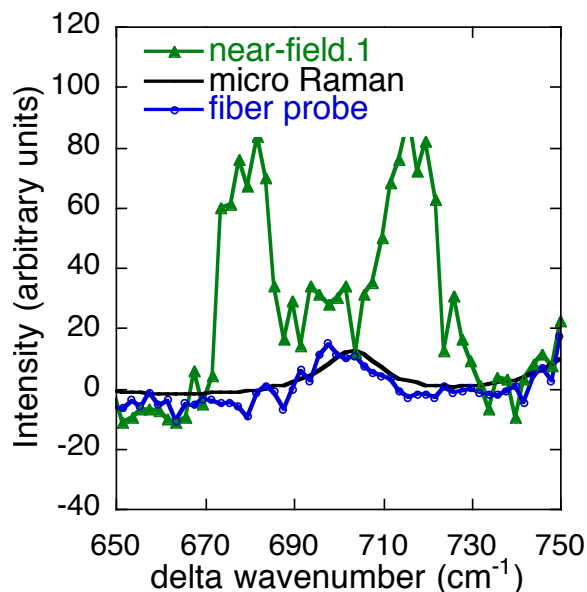


Figure 1: Scaled (to the peak at 767 cm^{-1}) Raman spectra for KTP showing differences between Near-field spectra, micro-Raman spectra, and far-field spectra through the probe.

tip angled away from the evaporation source so that an aperture is left uncoated. We have used fibers sharpened by the heat-and-pull method [28] and by etching. [29] Aluminum forms the aperture. The probe is positioned near the surface under lateral force feedback. [30] The NSOM is used in illumination mode, with 514 nm Ar ion laser light. Reflected light is collimated with a 0.50 NA lens [31], passed through a holographic filter to remove elastically scattered light, focussed into a single stage, 1 meter, Czerny-Turner spectrometer, and finally collected onto a cooled (-45 C) CCD camera. The light reflected from the holographic filter is collected and provides a reflection image which, combined with the simultaneous topography offered by the force feedback, corroborates a Raman image, if acquired. The primary difficulty encountered in NSOM-Raman is that of low signal levels. Input of more than a few milliwatts of light into the probe's fiber will destroy the probe tip. [32] Smaller tip apertures strongly reduce the probe throughput, [33] and Raman cross sections are relatively small. The aperture size directly controls the lateral resolution of the microscope.

We have taken comparative spectra of a KTP sample using micro-Raman, Raman with an NSOM probe retracted from the surface, and NSOM-Raman (in the near-field). [3-5, 34] Portions of these spectra are shown in Figure 1. The spectra have been normalized to the strong Raman peak at 767 cm^{-1} . The two far field spectra are the same to within noise, but the near-field spectrum differs by the apparent addition of peaks near 680 and 714 cm^{-1} . KTP has vibration energies at 683 and 712 cm^{-1} . The 683 line has been observed as a weak line in prior Raman work. [35] The 712 wavenumber vibration has been observed as a strong IR (not Raman) line. [36] Other NSOM-Raman studies of this system focussed on the probe (metal)-sample distance dependence of the line intensity. [37] The 683 cm^{-1} mode was not observed, but the 712 cm^{-1} mode was enhanced in the near field. The distance dependence, Figure 2, is consistent with the field gradient model. The Bethe-Bouwkamp model [38, 39] for NSOM fields is used to derive the expected GFR and standard Raman distance dependence in the figure. The GFR model provides a much better fit. Also, since the 712 cm^{-1} mode is strong in IR absorption, it is likely that the GFR effect is at least partially responsible for the spectra. The ratio of the Raman peak at 767 cm^{-1} to the GFR peak at 712 cm^{-1} is about 2 for the data in Figure 1, and ~ 200 for

butene on silver [27] has shown the presence of several out-of-plane modes, but not in-plane modes, when it lies on the surface. These are not present for molecules further from the surface, where the field gradients would be smaller.

Near-field scanning optical microscopy (NSOM), using a metal aperture at the probe tip to limit the illuminated area, provides another experimental configuration where GFR effects, including those of solid materials rather than molecules, may be observed. The metal that forms the aperture creates the strong field gradients that are required. This configuration has the advantage that the metal can be moved with high precision in all three dimensions. It can be scanned over a surface, permitting studies of adsorbed species or the solid substrate itself. Further, it can be retracted from the surface so as to move the high field gradient region away from the surface, effectively 'turning off' the GFR effect. This is an important test to confirm the origins of the observed Raman lines.

In NSOM, a sharpened optical fiber is coated with metal by rotating the probe with the tip angled away from the evaporation source so that an aperture is left uncoated. We have used fibers sharpened by the heat-and-pull method [28] and by etching. [29] Aluminum forms the aperture. The probe is positioned near the surface under lateral force feedback. [30] The NSOM is used in illumination mode, with 514 nm Ar ion laser light. Reflected light is collimated with a 0.50 NA lens [31], passed through a holographic filter to remove elastically scattered light, focussed into a single stage, 1 meter, Czerny-Turner spectrometer, and finally collected onto a cooled (-45 C) CCD camera. The light reflected from the holographic filter is collected and provides a reflection image which, combined with the simultaneous topography offered by the force feedback, corroborates a Raman image, if acquired. The primary difficulty encountered in NSOM-Raman is that of low signal levels. Input of more than a few milliwatts of light into the probe's fiber will destroy the probe tip. [32] Smaller tip apertures strongly reduce the probe throughput, [33] and Raman cross sections are relatively small. The aperture size directly controls the lateral resolution of the microscope.

that in Figure 2. These ratios compare well to those of a simple microscopic model based upon polarizabilities from the literature, [40] and polarizability gradients estimated from comparison of the long and short Ti-O bond data. The model gives a ratio of ~ 2.8 when the field gradient / field ratio is calculated for a flake on the tip (an edge 1 Å from the surface), and ~ 170 for the Bethe-Bouwkamp fields at 10 nm.

In summary, we have described a new mechanism by which a strong gradient of the electric field can cause normally forbidden vibration modes to appear in Raman spectra. The amplitude of the signal should be similar to that of the allowed Raman modes, and the relative strength of the modes should be similar to those in infrared spectroscopy, for IR allowed modes. Since infrared and Raman modes are complementary in many materials, this gradient-field Raman spectroscopy should help to provide a full vibrational analysis of a sample in a single measurement, especially when combined with an NSOM measurement, which allows the GFR terms to be preferentially reduced for positive identification of modes. The GFR effect is strongly dependent on the tip-sample distance. This results in a preferential sensitivity to surface rather than bulk effects, and raises the possibility of measuring Raman shifts of the surface, where the vibration levels inherently differ from the bulk.

We thank Philip Stiles, Suzanne Huerth, Michael Taylor, and Steve Winder for useful discussions or assistance. This work was supported by the U.S. Army Research Office through grant DAAH04-93-G-0194, the Office of Naval Research through grant N00014-98-1-0228 and the National Science Foundation through grant DMR-9975543.

References:

- [1] Martin Moskovits, Rev. Mod. Phys. **57**, 783 (1985).
- [2] J. A. Creighton, in *Spectroscopy of Surfaces*, Edited by R. J. H. C. a. R. E. Hester (John Wiley & Sons, New York, 1988) 37.
- [3] C.L. Jahncke, M.A. Paesler and H.D. Hallen, Appl. Phys. Lett. **67**, 2483 (1995).
- [4] C. L. Jahncke, H. D. Hallen and M. A. Paesler, J. of Raman Spectroscopy **27**, 579 (1996).
- [5] C.L. Jahncke and H.D. Hallen, Proceedings of 9th annual meeting of IEEE Lasers and Electro-Optics Society (LEOS) 96, **1**, 176 (1996).
- [6] M. Moskovits, J. Chem. Phys. **77**, 4408 (1982).
- [7] Max E. Lippitsch, Phys. Rev. B **29**, 3101 (1984).
- [8] Mary L. Patterson and Michael J. Weaver, J. Phys. Chem. **89**, 1331 (1985).
- [9] Alan Campion and David R. Mullins, Chem. Phys. Lett **94**, 576 (1983).
- [10] S. Buchner, E. Burstein and A. Pinczuk, Proceedings of 3rd International Conference on Light Scattering in Solids, Paris, France, Flammarion Sci **6 (10)**, xv (1976).
- [11] A. Pinczuk and E. Burstein, Solid State Commun **6**, 407 (1968).
- [12] F. Schäffler and G. Abstreiter, Phys. Rev. B **34**, 4017 (1986).
- [13] J.K. Sass, H. Neff, M. Moskovits and S. Holloway, J. Phys. Chem **85**, 621 (1981).
- [14] M. Moskovits and D.P. DiLella, J. Chem. Phys **77**, 1655 (1982).

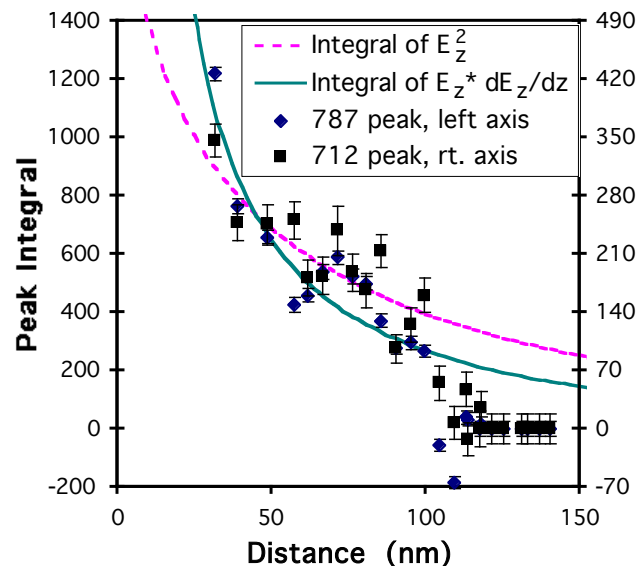


Figure 2: The points show the integral under the 712 cm^{-1} peak and that under the 787 cm^{-1} peak in difference spectra obtained by subtracting spectra at the distances indicated from those far from the surface. The solid line is a model for GFR as described in the text, and the dotted line is what would be expected for the standard Raman case.

- [15] A.M. Polubotko, *Physics Letters* **146**, 81 (1990).
- [16] Amnon Yariv, "Quantum Electronics," (Wiley, New York, 1975).
- [17] P.J. Feibelman, *Phys. Rev. B* **12**, 1319 (1975).
- [18] John R. Ferraro and Kazuo Nakamoto, "Introductory Raman Spectroscopy," (Academic Press, Boston, 1994).
- [19] E. Betzig and J.K. Trautman, *Science* **257**, 189 (1992).
- [20] M. Moskovits and D.P. DiLella, *J. Chem. Phys.* **73**, 6068 (1980).
- [21] P.A. Lund, R.R. Smardzewski and D.E. Tevault, *Chem. Phys. Lett* **89**, 508 (1982).
- [22] P.A. Lund, D.E. Tevault and R.R. Smardzewski, *J. Phys. Chem* **88**, 1731 (1984).
- [23] NIST Chemistry WebBook, <http://webbook.nist.gov>
- [24] Craig S. Allen and Richard P. van Duyne, *J. Am. Chem. Soc* **103**, 7497 (1981).
- [25] Kelly L. Akers, Lisa M. Cousins and Martin Moskovits, *Chem. Phys. Lett* **190**, 614 (1992).
- [26] Yun Zhang, Yuhua Du, John R. Shapley and Michael J. Weaver, *Chem. Phys. Lett* **205**, 508 (1993).
- [27] Daniel P. DiLella and Martin Moskovits, *J. Phys. Chem* **85**, 2042 (1981).
- [28] B.I. Yakobson, P.J. Moyer and M.A. Paesler, *J. Appl. Phys.* **73**, 7984 (1993).
- [29] P. Hoffmann, B. Dutoit and R.-P. Salathé, *Ultramicroscopy* **61**, 165 (1995).
- [30] Khaled Karrai and Robert D. Grober, *Applied Physics Letters* **66**, 1842 (1995).
- [31] Eric Ayars and H. D. Hallen, (unpublished).
- [32] A. H. LaRosa, B. I. Yakobson and H. D. Hallen, *Appl. Phys. Lett.* **67**, (1995).
- [33] B.I. Yakobson and M.A. Paesler, *Ultramicroscopy* **57**, 204 (1995).
- [34] H. D. Hallen, A. H. La Rosa and C. L. Jahncke, *Phys. Stat. Sol. (a)* **152**, 257 (1995).
- [35] Hua-guang Yang, Ben-yuan Gu, Yan-yun Wang, Huang Cheng-en and De-zhong Shen, *Guangxue Xuebac* **6**, 1071 (1986).
- [36] J. C. Jacco, *Materials Research Bulletin* **21**, 1189 (1986).
- [37] Eric Ayars and H.D. Hallen, *Appl. Phys. Lett.* (in press June 2000).
- [38] H.A. Bethe, *Physical Review* **66**, 163 (1944).
- [39] C.J. Bouwkamp, *Phillips Research Report* **5**, 401 (1950).
- [40] P.A. Thomas, *Materials for Non-linear and Electro-optics. Proceedings of the International Conference*, **59** (1989).